

The nanofluidics can explain ascent of water in tallest trees

Henri Gouin*

Abstract.

In *Amazing numbers in biology*, Flindt reports a giant, 128 meter-tall eucalyptus, and a 135 meter-tall sequoia¹. However, the explanation of the maximum altitude of the crude sap ascent and consequently the main reason of the maximum size that trees can reach is not well understood².

According to tree species, the crude sap is driven in xylem microtubes with diameters ranging between 50 and 400 micrometers. The sap contains diluted salts but its physical properties are roughly those of water; consequently, hydrodynamic, capillarity and osmotic pressure yield a crude sap ascent of a few tens of meters only³.

Today, we can propound a new understanding of the ascent of sap to the top of very tall trees thanks to a new comparison between experiments associated with the *cohesion-tension theory*⁴ and the *disjoining pressure concept*⁵.

Here we show that the pressure in the water-storing tracheids of leaves can be strongly negative whereas the pressure in the xylem microtubes of stems may remain positive when, at high level, inhomogeneous liquid nanolayers wet the xylem walls of microtubes. The nanofluidic model of crude sap in tall trees⁶ discloses a stable sap layer up to an altitude where the *pancake layer thickness*⁷ coexists with the dry xylem wall and corresponds to the maximum size of tallest trees. In very thin layers, sap flows are widely more significant than those obtained with classical Navier-Stokes models and consequently are able to refill stomatic cells when phloem embolisms supervene.

These results drop an inkling that the disjoining pressure is an efficient tool to study biological liquids in contact with substrates at a nanoscale range.

The most classical explanation of the sap ascent phenomenon in tall trees is given by the cohesion-tension

*henri.gouin@univ-amu.fr

M2P2, C.N.R.S. U.M.R. 7340 & Université d'Aix-Marseille, Avenue Escadrille Normandie-Niemen, 13397 Marseille Cedex 20 France

theory propounded in 1894 by Dixon and Joly⁴, followed by a quantitative analysis of the sap motion proposed by van der Honert in 1948⁸: According to this theory, the crude sap fills water-tight microtubes of dead xylem cells and its transport is due to a gradient of negative pressure producing the traction necessary to lift water against gravity. A main experimental checking on the cohesion-tension theory comes from an apparatus called *Scholander pressure chamber* (see Fig. 1). The decrease in the negative pressure is related to the

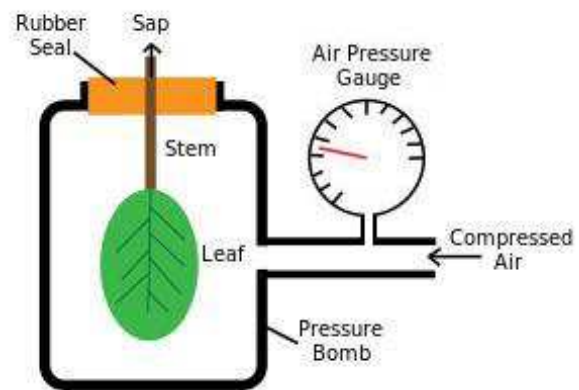


Figure 1: Sketch of the Scholander pressure chamber (or Scholander pressure bomb)⁹. A leaf attached to a stem is placed inside a sealed chamber. Compressed air is slowly added to the chamber. As the pressure increases to a convenient level, the sap is forced out of the xylem and is visible at the cut end of the stem. The required pressure is opposite and of equal magnitude to the water pressure in the water-storing tracheids in the leaf.

closing of the aperture of microscopic stomata in leaves through which water vapour is lost by transpiration.

Nonetheless, several objections question the cohesion-tension theory:

We first refer to the well-known book by M.H. Zimmermann³. He said: "The heartwood is referred to as a wet wood. It may contain liquid under positive pressure while in the sapwood the transpiration stream moves along a gradient of negative pressures. Why is the water of the central wet core not drawn into the sapwood? Free water, i.e. water in tracheids, decreases in successively older layers of wood as the number of embolized tracheids increases. The heartwood is relatively dry i.e. most tracheids are embolized. It is rather ironic that a wound in the wet wood area, which bleeds liquid for a long period of time, thus appears to have the transpiration stream as a source of water, in spite of the fact that the pressure of the transpiration stream is negative most of the time! It should be quite clear by now that a drop in xylem pressure below

a critical level causes cavitations and normally puts the xylem out of function permanently. The cause of such a pressure drop can be either a failing of water to the xylem by the roots, or excessive demand by transpiration.”

At great elevation in trees, the value of the negative pressure increases the risk of cavitation and consequently, the formation of embolisms may cause a breakdown of the continuous column of sap inducing the leaf death. The crude sap is a liquid bulk with a superficial tension σ lower than the superficial tension of pure water which is about 72.5 cgs at 20° Celsius; if we consider a microscopic gas-vapour bubble with a diameter $2R$ smaller than xylem microtube diameters, the difference between the gas-vapour pressure and the liquid sap pressure is expressed by the Laplace formula $P_v - P_l = 2\sigma/R$; the vapour-gas pressure is positive and consequently unstable bubbles must appear when $R \geq -2\sigma/P_l$. For a negative pressure $P_l = -0.6$ MPa in the sap, we obtain $R \geq 0.24 \mu m$; then, when all the vessels are tight filled, germs naturally pre-existing in crude water may spontaneously embolize the tracheids. Haberlandt¹⁰ described water-storing tracheids in leaves; they are roundish in shape, and located either at the tips of the veins or detached from transporting xylem. In more recent papers they have been called *tracheid idioblats*¹¹. The spacing considered in Pridgeon’s paper¹² is about $2 \mu m$ or less at the top of trees as suggested on Fig. 2 of the paper by Koch *et al*² and has a good size to prevent cavitation for nucleus germs of the same order of magnitude.

No vessels are continuous from root to stem, from stem to shoot, and from shoot to petiole. The vessels do not all run neatly parallel and form a network generally up a few centimeters long. The ends usually taper out; it is very important for the understanding of water conduction to realize that the water does not leave a vessel in axial direction through the very end but laterally along a relatively long stretch where the two vessels, the ending and the continuing ones, run side by side.

The vascular bundles of some leaves are surrounded by a bundle sheath, containing a suberized layer comparable to the one of the Casperian strip in the roots¹³. This seal separates the apoplast into two compartments, one inside and the other one outside the bundle sheath. The two areas are only connected by the plasmodesmata that connect living cells. The pressure in the intact, water-containing neighbouring tracheids, may still be negative; a considerable pressure drop therefore exists across the pit membranes. Pressure chamber measurements cannot be considered as pressure values of the stem xylem without special precautions, simply because they are taken elsewhere.

Hydraulically then, the leaf is very sharply separated from the stem. The wet wood area of elms appears to act like a single, giant osmotic cell that is separated from the sapwood area by a semi permeable membrane. This can be visualized somewhat like a Traube membrane, as early plant physiologists called it¹⁴.

Another objection in the perfect confidence to the cohesion-tension theory was the experiments by Preston¹⁵ who demonstrated that tall trees survived by overlapping double saw-cuts made through the cross-sectional area of the trunk to sever all xylem elements. This result, confirmed by several authors (e.g.¹⁶), does not seem in agreement with the possibility of strong negative pressures in the water-tight microtubes. Using a xylem pressure probe, Balling *et al*¹⁷ showed that, in many circumstances, this apparatus does not measure any water tension¹⁸.

As a consequence of these various pieces of evidence, the main question is:

The negative pressure measured by the Sholander pressure chamber being the pressure in the water-storing tracheids, is it possible that the pressure in the xylem microtubes of the stem remains positive?

A positive answer to this question comes from the concept of disjoining pressure which is able to interpret very thin vertical films of liquid wetting solid substrates. The simplest review relative to the disjoining pressure is presented in the well-known monograph by Derjaguin *et al*⁵. An apparatus measuring the disjoining pressure denoted Π is due to Sheludko¹⁹. The apparatus is schematically described on Fig. 2 and allows to understand the disjoining pressure concept. Fluids and solids are at the same temperature. The film is thin enough for the gravity effect across the layer to be neglected. The hydrostatic pressure in a thin liquid layer included between a solid substrate and a vapour-gas bulk differs from the pressure in the liquid bulk contained in the reservoir. The forces arising from the thinning of a film of uniform thickness h yield the disjoining pressure as a function of h ($\Pi = \Pi(h)$). The disjoining pressure is equal to the difference between the pressure P_{v_b} through the interfacial surface of the thin liquid layer (which is the total pressure of gases and *vapour bulk*) and the pressure P_{l_b} at the top of the liquid bulk with dissolved gases contained in the reservoir from which the thin liquid layer extends:

$$\Pi = P_{v_b} - P_{l_b}.$$

As a vapour-gas pressure, the pressure P_{v_b} is always positive; depending on H-values, the pressure P_{l_b} may be negative.

These comments illuminate an original comparison

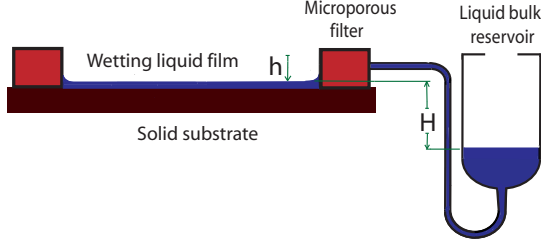


Figure 2: **The Sheludko apparatus** . Schematic diagram of the technique to determine the disjoining pressure isotherms of wetting films on a solid substrate: a circular wetting film is formed on a flat substrate to which a microporous filter is clamped. A pipe connects the filter filled with the liquid to a reservoir containing the liquid bulk that can be moved by a micrometric device. The disjoining pressure is equal to $\Pi = (\rho_{l_b} - \rho_{v_b})gH$, where g is the acceleration of gravity and ρ_{l_b} , ρ_{v_b} are the densities in the liquid and the vapour-gas bulks, respectively (From⁵ page 332).

between the Sholander pressure chamber experiment presented in Fig. 1 and the apparatus proposed by Sheludko in Fig. 2 and make a total change in the interpretation of Sholander pressure chamber data for the tallest trees:

In the Sholander pressure chamber, the cohesion-tension theory assumes that, at a given level, liquids entirely convey the pressure as is the case for incompressible fluids. This assumption is for thin layers at odds with the Sheludko experiment where the disjoining pressure highlights a strong difference between liquid bulk and thin layer pressures. The xylem of stem walls is associated with the solid substrate and the water-storing tracheids in leaves are associated with the liquid bulk reservoir of Sheludko's experiment.

In our new interpretation, the negative pressure measured in the Sholander pressure chamber is the pressure in water-storing tracheids corresponding to the liquid bulk reservoir of Sheludko while the pressure in the xylem microtubes of stems remains positive as in the wetting thin layer of Sheludko's experiment when H -value is equal to the level in the tree.

As proven in⁵, Chapter 2, the Gibbs free energy per unit area of the liquid layer denoted G can be expressed as a function of h thanks to the relation:

$$G(h) = \int_h^{+\infty} \Pi(u) du,$$

where $h = 0$ is associated with a dry wall in contact with the vapour-gas bulk and $h = +\infty$ is associated with a wall in contact with the liquid bulk when the value of G is equal to 0. The coexistence of two film seg-

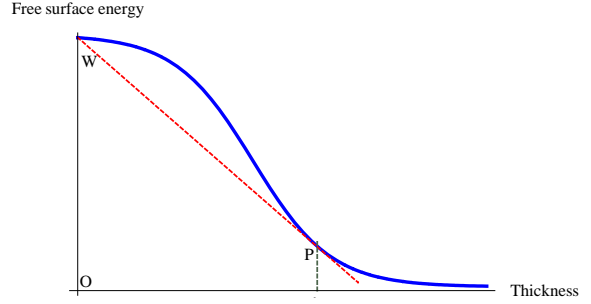


Figure 3: **The pancake layer thickness** . The construction of the tangent to curve $G(h)$ issued from point W of coordinates $(0, G(0))$ yields point P; point W is associated with a high-energy surface of the dry wall and point P is associated with the pancake thickness h_p ⁷ .

ments with different thicknesses is a phenomenon which can be represented by the equality of chemical potential and superficial tension of the two films⁵ . A spectacular case corresponds to the coexistence of a liquid film of thickness h_p and the dry solid wall; the liquid film is the so-called pancake layer and corresponds to the minimal thickness for which a stable wetting film damps a solid wall^{5,7} . This minimal thickness h_p verifies:

$$G(0) = G(h_p) + h_p \Pi(h_p). \quad (1)$$

The geometrical interpretation of Eq. (1) is proposed on Fig. 3.

Now, we consider a film of thickness h_x at level x . Only liquid water films of thicknesses $h_x > h_p$ are stable. The disjoining pressure of the mixture of water and perfect gas is the same as for a single liquid far under its critical point^{5,6} . Calculations limited to overstrained liquid layers of a few nanometers thick yield the disjoining pressure in the approximated form^{20,21} :

$$\begin{aligned} \Pi(h_x) \simeq & \frac{2c_l^2}{\rho_l} \left[(\gamma_1 - \gamma_2 \rho_l)(\gamma_2 + \gamma_3)e^{h_x \tau} + (\gamma_2 - \gamma_3)\gamma_2 \rho_l \right] \\ & \times \frac{[(\gamma_2 + \gamma_3)\gamma_2 \rho_l + (\gamma_1 - \gamma_2 \rho_l)(\gamma_2 - \gamma_3)e^{-h_x \tau}]}{[(\gamma_2 + \gamma_3)^2 e^{h_x \tau} - (\gamma_2 - \gamma_3)^2 e^{-h_x \tau}]^2}, \quad (2) \end{aligned}$$

where ρ_l is the liquid density in normal conditions, c_l is the isothermal sound velocity in the liquid water bulk, γ_1 , γ_2 , γ_3 and τ are positive constants given by the mean field molecular theory^{22,23} :

$$\begin{aligned} \gamma_1 &= \frac{\pi c_{ls}}{12\delta^2 m_l m_s} \rho_{sol}, & \gamma_2 &= \frac{\pi c_{ll}}{12\delta^2 m_l^2}, \\ \gamma_3 &= c_l \sqrt{\frac{2\pi c_{ll}}{3\sigma_l m_l^2}}, & \tau &= c_l \sqrt{\frac{3\sigma_l m_l^2}{2\pi c_{ll}}}. \end{aligned}$$

Constants c_{ll} and c_{ls} are associated with Hamaker coefficients of interaction of liquid *vs* liquid and liquid *vs* solid²⁴; σ_l denotes the fluid molecular diameter and $\delta = \frac{1}{2}(\sigma_l + \sigma_s)$, where σ_s denotes the solid molecular diameter; m_l , m_s denote the masses of fluid and solid molecules; ρ_{sol} denotes the solid density. Expression (2) differs from Lifshitz's relation²⁵ where the disjoining pressure of microscopic layers of liquid, assumed to be incompressible, has a behavior in the form $\Pi(h) \sim h^{-3}$. To obtain the pancake thickness corresponding to the smallest thickness of the liquid layer, we draw the graphs of $G(h_x)$ and $\Pi(h_x)$ when $h_x \in [(1/2)\sigma_l, \ell]$, where ℓ is a length of a few tens of ångströms. Let us note that $d = 1/\tau$ is the natural reference length scale. For a few nanometers, the film thickness is not exactly h_x ; we must add the thickness estimated at $2\sigma_l$ of the liquid part of the liquid-vapour interface bordering the liquid layer and the nanolayer thickness is approximately $e_x \approx h_x + 2\sigma_l$ ²².

Our aim is now to point out a numerical example such that previous results provide a value of maximum height for a vertical water film wetting a wall of xylem. We considered water at 20° Celsius. The experimental estimates of coefficients are expressed in c.g.s. units^{24,26}: $\rho_l = 0.998$, $c_l = 1.478 \times 10^5$, $c_{ll} = 1.4 \times 10^{-58}$, $\sigma_l = 2.8 \times 10^{-8}$, $m_l = 2.99 \times 10^{-23}$. We deduce $\gamma_2 = 54.2$, $\gamma_3 = 506$, $d = 2.31 \times 10^{-8}$. We consider the Young contact angle between the xylem wall and the liquid-vapour water interface as $\theta \approx 50^\circ$ (this value is an arithmetic average of different Young angles proposed in the literature²⁷). Coefficients c_{ls} and γ_1 can be obtained from the substrate-liquid surface free energy expressed in the form^{7,23}:

$$\phi(\rho_s) = -\gamma_1 \rho_s + \frac{1}{2} \gamma_2 \rho_s^2.$$

Here $\rho_s \simeq \rho_l$ denotes the fluid density value at the surface; from the superficial tension σ and Young's condition, we immediately get $\gamma_1 \approx 75$ (21). In the upper graph of Fig. 4 we present the free energy graph $G(h_x)$. Due to $h_x > (1/2)\sigma_l$, it is not numerically possible to obtain the limit point W corresponding to the dry wall; point W is obtained by an interpolation associated with the concave part of the G -curve. Point P follows from the drawing of the tangent line issued from W to the G -curve. In the lower graph of Fig. 4 we present the disjoining pressure graph $\Pi(h_x)$. The physical part of the disjoining pressure graph corresponding to $\partial\Pi/\partial h_x < 0$ is associated with a liquid layer of several molecules thick. The part $\partial\Pi/\partial h_x > 0$ is also obtained by Derjaguin *et al*⁵. The reference length d is of the same order as σ_l and is a good length unit for very thin films. The total pancake thickness e_p is of one nanometer order corresponding to a good thickness

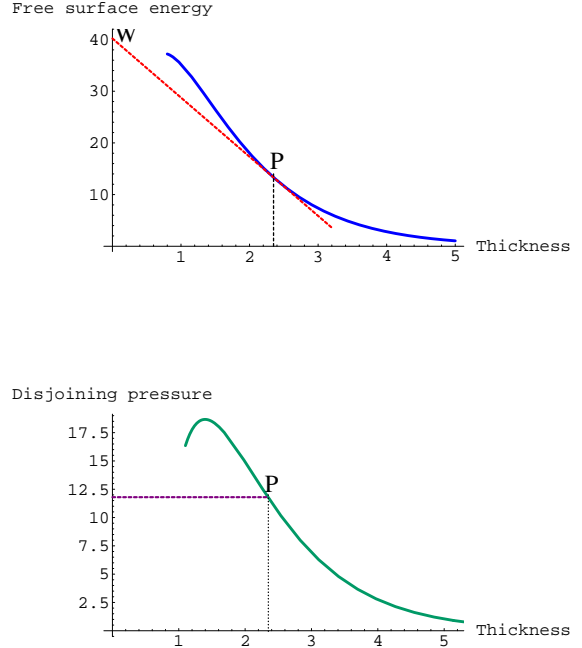


Figure 4: **The maximum height of trees**. *Upper graph*: $G(h_x)$ -graph. The unit of x -axis graduated by h_x is $d = 2.31 \times 10^{-8}$ cm; the unit of y -axis is one c.g.s. unit of surface tension. *Lower graph*: $\Pi(h_x)$ -graph. The unit of x -axis graduated by h_x is $d = 2.31 \times 10^{-8}$ cm; the unit of y -axis is one atmosphere.

value for a high-energy surface^{7,24}; consequently in the tall trees, at high level, the thickness of the layer is of a few nanometers. The point P of the lower graph corresponds to the point P of upper graph. Let us note that the crude sap is not pure water; its liquid-vapour surface tension has a lower value than the surface tension of pure water and it is possible to obtain the same spreading coefficients with less energetic surfaces.

When x_p corresponds to the altitude of the pancake layer, $\Pi \simeq \rho_l g x_p$ ^{5,20}. To this altitude, we add 20 meters corresponding to the ascent of sap due to capillarity and osmotic pressure and we obtain on the lower graph of Fig. 4 a maximum film height of approximately 140 meters (20 + 120 meters) corresponding to 12 atmospheres, which is of the same level order as the topmost trees.

These results arising from molecular physics require a comparison between the behaviours of liquid motions

both in microtubes and in nanolayers :

When the xylem microtubes are tight filled with crude sap, the liquid motions are Poiseuille flows³ and to be efficient the microtube radii should be as wide as possible, which is not the case. Due to the liquid incompressibility the flow is *very rigid* and the pressure effects are fully propagated onto the microtube walls.

When the xylem microtubes are partially filled with thin water films, there are qualitative experiments for slippage on the walls when the film thickness is of the mean free path order^{28,29}; the boundary condition on the walls writes:

$$\mathbf{u} = L_s \, d\mathbf{u}/dn,$$

where \mathbf{u} is the liquid velocity, $d\mathbf{u}/dn$ is the normal derivative at the wall and L_s is the so-called *Navier length*²⁹. The Navier length may be as large as a few microns³⁰ and we obtained the mean liquid velocity $\bar{\mathbf{u}}$ along a thin layer from²¹:

$$\nu \bar{\mathbf{u}} = h_x \left(\frac{h_x}{3} + L_s \right) [\mathbf{grad} \Pi(h_x) - g \mathbf{i}], \quad (3)$$

where ν denotes the kinematic viscosity and \mathbf{i} the unit vertical vector. Consequently the slippage condition multiplies the flow rate by a factor of $(1 + 3L_s/h_x)$. For example, if $h_x = 3 \, nm$ and $L_s = 100 \, nm$, which is a Navier length of small magnitude with respect to experiments, the multiplicative factor is 10^2 ; if $L_s = 7 \, \mu m$, as considered in³⁰, the multiplicative factor is 10^4 which is of the same order as for nanotube observations²⁷. Equation (3) is mainly realistic at the top of tallest trees where the xylem network is strongly ramified; the heartwood may contain liquid under positive pressure and is connected with the sapwood³. The flow rate can increase or decrease due to the spatial derivative of the thickness h_x and consequently depends on the local disjoining pressure value. The tree's versatility adapts the disjoining pressure gradient effects by opening or closing the stomatic pits, so that the bulk pressure in micropores can be more or less negative and so, the transport of water is differently dispatched in the stem parts.

The sap motion is induced by the transpiration across micropores located in tree leaves³. It seems natural to surmise that the diameters of xylem microtubes might result of a competition between evaporation which reduces the flow of sap and the flux of transpiration in micropores inducing the motion. It is noticeable that if we replace the flat surfaces of the microtubes with wedge geometry or corrugated surface, it is much easier to obtain the complete wetting requirement; thus, plants can avoid having very high energy surfaces. Nonetheless, they are still internally wet if crude sap flows through

wedge shaped corrugated pores. The wedge does not have to be perfect on the nanometric scale to significantly enhance the amount of liquid flowing at modest pressures, the walls being considered as plane surfaces endowed with an average surface energy.

Methods.

We compare two experiments:

- *The Scholander pressure bomb experiment (1955) based on the cohesion-tension theory (1894) in which liquids are considered to be incompressible.*

- *The Sheludko experiment (1967) based on the concept of disjoining pressure in DLVO theory (1948) that highlights a strong difference between liquid bulk and thin layer pressures.*

The theoretical results allow us to obtain:

- *The computation of tallest trees' level that fits with real facts.*

- *The interpretation of the motion in xylem microtubes by using the shallow water approximation and the slippage on walls at the nanometric scale.*

References

- [1] Flindt, R. *Amazing Numbers in Biology* (Springer, New York, 2006).
- [2] Koch, W., Sillett, S.C., Jennings, G.M. & Davis S.D. The limit to tree height. *Nature* **428**, 851-854 (2004).
- [3] Zimmermann, M.H. *Xylem Structure and the Ascent of Sap* (Springer, New York, 1983).
- [4] Dixon, H.H. & Joly, J. On the ascent of sap. *Philosophical Transactions of the Royal Society of London, B* **186**: 563-576 (1894).
- [5] Derjaguin, B.V., Churaev, N.V. & Muller, V.M. *Surfaces Forces* (Plenum Press, New York, 1987).
- [6] Gouin, H. A mechanical model for the disjoining pressure, *International Journal of Engineering Science* **47**, 691-699 (2009) & arXiv:0904.1809.
- [7] de Gennes, P.G. Wetting : statics and dynamics. *Review of Modern Physics* **57**, 827-863 (1985).
- [8] van der Honert, T.H. Water transport in plants as a catenary process. *Discussions of the Faraday Society* **3**, 1105-1113 (1948).
- [9] Scholander, P.F., Love, W.E. & Kanwisher, J.W. The rise of sap in tall grapevines. *Plant Physiology* **30**, 93-104 (1955).
- [10] Haberlandt, G. *Physiological plant anatomy* (MacMillan, London, 1914).
- [11] Foster, A.S. Plant idioblast: remarkable examples of cell specialization. *Protoplasma* **46**, 183-193 (1956).
- [12] Pridgeon, A.M. Diagnostic anatomical characters in the pleurothallidinae (orchidaceae). *American Journal of Botany* **69**, 921-938 (1982).

- [13] O'Brien, T.P. & Carr, D.J. A suberized layer in the cell walls of the bundle sheath of grasses. *Australian Journal of Biological Science* **23**, 275-287 (1970).
- [14] Traube, M. Experimente zur Theorie der Zellenbildung und Endosmose. *Archiv für Anatomie, Physiologie und wissenschaftliche Medizin*, Berlin **34**, 87-165 (1867).
- [15] Preston, R.D. In: Deformation and Flow in Biological Systems (ed. Frey-Wyssling, A.) 257-321, (North Holland Publishing, Holland, 1952).
- [16] Mackay, J.F.G. & Weatherley, P.E. The effects of transverse cuts through the stems of transpiring woody plants on water transport and stress in the leaves. *Journal of Experimental Botany* **24**, 15-28 (1973).
- [17] Balling, A. & Zimmermann, U. Comparative measurements of the xylem pressure of nicotiana plants by means of the pressure bomb and pressure probe. *Planta* **182**, 325-338 (1990).
- [18] Tyree, M.T., Cochard, H. & Cruiziat, P. The water-filled versus air-filled status of vessels cut open in air: The 'Scholander assumption' revisited. *Plant, Cell & Environment* **26**, 613-621 (2003).
- [19] Sheludko, A. Thin liquid films. *Advance in Colloid Interface Science* **1**, 391-464 (1967).
- [20] Gouin, H. A new approach for the limit to tree height using a liquid nanolayer model. *Continuum Mechanics and Thermodynamics* **20**, 317-329 (2008) & arXiv:0809.3529.
- [21] Gouin, H. Solid-liquid interaction at nanoscale and its application in vegetal biology. *Colloids and Surfaces A* **383**, 17-22 (2011) & arXiv:1106.1275.
- [22] Rowlinson J.S. & Widom, B. *Molecular Theory of Capillarity* (Clarendon Press, Oxford, 1984).
- [23] Gouin, H. Energy of interaction between solid surfaces and liquids. *The Journal of Physical Chemistry B* **102**, 1212-1218 (1998) & arXiv:0801.4481.
- [24] Israelachvili, J. *Intermolecular Forces* (Academic Press, New York, 1992).
- [25] Dzyaloshinsky, I.E., Lifshitz, E.M. & Pitaevsky, L.P. The general theory of van der Waals forces, *Advances in Physics* **10**, 165-209 (1961).
- [26] Weast, R.C. (ed.) *Handbook of Chemistry and Physics* 65th Edition (CRC Press, Boca Raton, 1984).
- [27] Mattia, D. & Gogotsi, Y. Review: static and dynamic behavior of liquids inside carbon nanotubes, *Microfluid Nanofluid* **5**, 289-305 (2008).
- [28] Chuarev, N.V. Thin liquid layers, *Colloid J.* **58**, 681-693 (1996).
- [29] de Gennes, P.G. On the fluid/wall slippage, *Langmuir* **8**, 3413-3414 (2002) & arXiv:0115383.
- [30] Tabeling, P. (ed.) Microfluidics, *Comptes Rendus Physique*, **5**, 2-608 (2004).